Inorganic Chemistry

Article

pubs.acs.org/IC

Luminescent P-Chirogenic Copper Clusters

Antony Lapprand,[†] Mathieu Dutartre,[‡] Naïma Khiri,[‡] Etienne Levert,[†] Daniel Fortin,[†] Yoann Rousselin,[‡] Armand Soldera,[†] Sylvain Jugé,*[,‡] and Pierre D. Harvey*[,†,‡]

[†]Département de Chimie, Université de Sherbrooke, 2500 Boul. Université, Sherbrooke, Québec, Canada J1K 2R1

[‡]Institut de Chimie Moléculaire de l'Université de Bourgogne (ICMUB, UMR 6302), Université de Bourgogne, Dijon, France

Supporting Information

ABSTRACT: P-chirogenic clusters of the cubanes $[Cu_4I_4L_4]$ (L = chiral phosphine) were prepared from (+)- and (−)-ephedrine with L = (*S*)- or (*R*)-(R)(Ph)(*i*-Pr)P (with R = CH_3 (seven steps) or $C_{17}H_{35}$ (10 steps)) with e.e. up to 96%. The X-ray structure of $[Cu_4I_4((R)\text{-}(CH_3)(Ph)(i\text{-}Pr)P)_4]$ confirmed the cubane structure with average Cu···Cu and Cu···I distances of 2.954 and 2.696 Å, respectively. The cubane structure of the corresponding $[Cu_4I_4((S)\text{-}(CH_3)(Ph)(i\text{-}Pr)P)_4]$ was established by the comparison of the X-ray powder diffraction patterns, and the opposite optical activity of the (*S*)- and (*R*)-ligand-containing clusters was confirmed by circular dichroism spectroscopy. Small-angle X-ray scattering patterns of one cluster bearing a $C_{17}H_{35}$ chain exhibit a weak signal at $2\theta \sim 2.8°$ ($d \sim 31.6$ Å), indicating some molecular ordering in the liquid state. The emission spectra exhibit two emission bands, both associated with triplet excited states. These two bands are assigned as follows: the high energy emission is due to a halide-to-ligand charge transfer, XLCT, state mixed with LXCT (ligand-to-halide-charge-transfer). The low energy band is assigned to a cluster-centered excited state. Both emissions are found to be thermochromic with the relative intensity changing between 77 and 298 K for the clusters in methylcyclohexane solution. Several differences are observed in the photophysical parameters, emission quantum yields and lifetimes for R = CH_3 and $C_{17}H_{35}$. The measurements of the polarization along the emission indicate that the emission is depolarized, consistent with an approximate tetrahedral geometry of the chromophores.

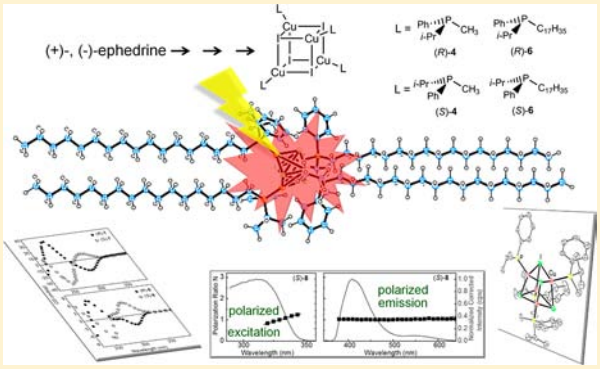

INTRODUCTION

Copper(I) catalyzed coupling reactions for carbon−carbon and carbon−heteroatom bond formation have greatly improved synthesis methodologies, motivated by environmental and economic reasons.[1,2] The asymmetric versions of these reactions based on chiral ligated copper salts or copper hydrides have also achieved high enantioselectivities.[3] The copper transmetalation from various organometallic reagents also contribute to the stereoselective reactions notably in the case of functionalized substrates.[4] Most chiral copper(I) complexes are prepared from phosphorus ligands bearing the chirality on the carbon in the backbone.[5,6] The interest in phosphine ligands bearing the chirality on the phosphorus atom (P-chirogenic) greatly expanded recently, due to the development of new stereoselective methods based on the borane complex chemistry.[6−8] Surprisingly, only a few chiral copper(I) catalyzed reactions are described using a P-chirogenic phosphorus ligand.[7] Yet their use in asymmetric catalysis presents much interest due to their structural design, which is relatively accessible.[6−8] P-chirogenic ligands are also interesting due to the possibility that the chirality can be bared by both the phosphorus and carbon atoms, thereby increasing the number of stereoisomers.[6,9] To the best of our knowledge, no P-chirogenic copper complexes have been described so far. Copper(I) halides display a wide diversity of complexes with phosphines either as mono- or multinuclear forms where the coordination number ranges from 2 to 4.[10] Moreover, the tetra(copper(I) iodide) clusters, $[Cu_4I_4L_4]$ (L = organic ligand), are particularly appealing because of their rich photoluminescence properties, which can be exploited to access materials exhibiting original optical properties, including thermochromic luminescence.[11] One of the key features is the presence of two emissions arising from cluster-centered (CC*, i.e. within the Cu_4X_4 skeleton) and halide-to-ligand charge transfer (XLCT) for the low and high energy bands, respectively. We now report the synthesis, the X-ray structure, and the photonic properties of the first examples of tetracopper iodide clusters bearing both enantiomers of P-chirogenic phosphines, **4** and **6** (Chart 1). These clusters are found to be strongly luminescent and thermochromic in solution.

EXPERIMENTAL SECTION

Materials and General Procedure. All reactions were carried out under an argon atmosphere in dried glassware with magnetic stirring. Solvents were dried prior to use. Tetrahydrofuran (THF) and toluene were distilled from sodium/benzophenone and stored under argon.

Received: February 26, 2013
Published: June 24, 2013

   dx.doi.org/10.1021/ic400498j | *Inorg. Chem.* 2013, 52, 7958−7967

Chart 1

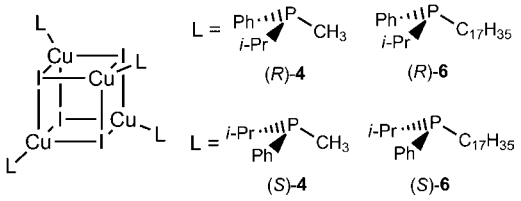

Dichloromethane (CH_2Cl_2) was distilled from CaH_2. Hexane and propan-2-ol for HPLC were of chromatographic grade and used without further purification. Isopropyllithium (0.7 M in pentane), methyllithium (1.6 M in Et_2O), *n*-butyllithium (2.5 M in hexane), 1-bromo-hexadecane ($C_{16}H_{33}Br$), 1,4-diazabicyclo[2.2.2]octane (DABCO), $BH_3{\cdot}SMe_2$, and $K_2[PtCl_4]$ were purchased from Aldrich, Acros, or Alfa Aesar and used as received. (+)- and (−)-Ephedrine were purchased from Aldrich and dried by azeotropic shift of toluene on a rotary evaporator. (2*R*,4*S*,5*R*)-(+)-3,4-Dimethyl-2,5-diphenyl-1,3,2-oxazaphospholidine-2-borane (**1**) and its enantiomer (2*S*, 4*R*, 5*S*)-(−)-**1** were prepared from appropriate (−)- or (+)-ephedrine, as previously described.[12] (R_p)-(+)-*N*-Methyl-*N*-[(1*S*,2*R*)(1-hydroxy-2-methyl-1-phenyl-2-propyl)]amino-*i*-propyl phenyl phosphine borane (**2**) and (*S*)-(+)-methylphenyl-*i*-propylphosphine borane (**3**) were prepared from (−)-ephedrine according to the published procedure.[12] The toluene HCl solution was obtained by bubbling HCl gas, and the resulting solution was titrated before use. Reactions were monitored by thin-layer chromatography (TLC) using 0.25-mm E. Merck precoated silica gel plates. Visualization was accomplished with UV light and/or appropriate staining reagents. Flash chromatography was performed with the indicated solvents using silica gel 60 (particle size 35−70 μm; Acros) or aluminum oxide 90 standardized (Merck).

(*R*)-Methylphenyl-*i*-propylphosphine (4; Prepared Using (−)-Ephedrine).[12a] In a 50 mL two-necked flask equipped with a magnetic stirrer and an argon inlet, 0.18 g of (*R*)-(−)-methylphenyl-*i*-propylphosphine borane (**3**; 1.0 mmol) and 0.56 g of DABCO (5 mmol) were dissolved in 10 mL of toluene. The reaction mixture was heated at 50 °C for 12 h. After cooling, the crude product was rapidly transferred via canula into a column previously evacuated and filled with argon containing neutral alumina. The reaction solution was filtered using degassed 9:1 toluene/ethyl acetate as the eluent. After removal of the solvent under a vacuum, 0.11 g of the free phosphine was obtained as a colorless oil. Yield: 65%. Colorless oil. ^{1}H NMR ($CDCl_3$, 600 MHz): δ 7.52−7.46 (m, 2H, CH_{arom}), 7.37−7.31 (m, 3H, CH_{arom}), 1.78 (m, 1H, C*H*), 1.30 (d, 3H, J = 3.0 Hz, PCH_3), 1.06 (dd, 3H, J = 13.6, 7.0 Hz, CH_3, *i*-Pr), 0.93 (dd, 3H, J = 14.9, 7.0 Hz, CH_3, *i*-Pr). ^{31}P NMR ($CDCl_3$, 121 MHz): δ −19.2.

The enantiomeric purity of (*R*)-**4** (>94% e.e.) was checked by comparison with a racemic sample, by ^{31}P NMR in the presence of (+)-di-μ-chlorobis{2[1-(dimethylamino)ethyl]phenyl-C,N}-dipalladium. ^{31}P NMR ($CDCl_3$, 121 MHz): δ +30.2 [(*R*)-enantiomer].

(*S*)-Methylphenyl-*i*-propylphosphine (4). This enantiomer was prepared using a similar procedure as for (*R*)-**4**, but using (+)-ephedrine.[12a] The enantiomeric excess of (*S*)-**4** was checked by comparison with a racemic sample, by ^{31}P NMR in the presence of (+)-di-μ-chlorobis{2[1-(dimethylamino)ethyl]phenyl-C,N}-dipalladium. ^{31}P NMR ($CDCl_3$, 121 MHz): δ +28.3 [(*S*)-enantiomer)].

(*R*)-(−)-Heptadecylphenyl-*i*-propylphosphine Borane (5). This compound was prepared using (−)-ephedrine, and the NMR characterization data are identical to those previously described.[9f] HRMS calcd for $C_{26}H_{50}BNaP$: $[M + Na]^+$ = 427.36401. Found: 427.36763. Anal. calcd for $C_{26}H_{50}BP$ (404.47): C, 77.21; H, 12.46. Found: C, 77.00; H, 12.60.

(*S*)-Heptadecylphenyl-*i*-propylphosphine Borane (5). This enantiomer was prepared using a similar procedure to that for (*R*)-**5**, but using (+)-ephedrine. The NMR and mass spectra are identical to the (*R*)-**5** described.[9f]

(*R*)-Heptadecylphenyl-*i*-propylphosphine (6). This compound was prepared using (−)-ephedrine, and the NMR characterization data are identical as previously described.[9f]

(*S*)-Heptadecylphenyl-*i*-propylphosphine (6). This enantiomer was prepared using a similar procedure as for (*R*)-**6** but using (+)-ephedrine. The NMR and mass spectra are identical to the (*R*)-**6** described.[9f]

Preparation of the Copper Complexes 7 and 8. *Tetrameric-[iodo(methylphenyl-i-propylphosphine)copper(I)]-(R_P)-**7**.* In a 50 mL two-necked flask equipped with a magnetic stirrer and an argon inlet, 0.17 g of (*R*)-phosphine **4** (1.0 mmol) and 0.19 g of CuI (1.0 mmol) were dissolved in 5 mL of toluene. The reaction mixture was heated at 60 °C overnight (a white solid appears). The solid is filtered on Millipore and washed with toluene to remove the excess copper. The solvent is evaporated, and the residue is triturated in methanol to afford 0.27 g of the desired complex as a white solid. Yield: 75%. White solid. $[\alpha]_D^{25}$ = −49.5 (c 1.0, $CHCl_3$). Mp = 143 °C. ^{1}H NMR ($CDCl_3$, 500 MHz): δ 7.75 (m, 2H, CH_{arom}), 7.31 (m, 3H, CH_{arom}), 2.14 (m, 1H, C*H*, *i*-Pr), 1.52 (d, 3H, J = 5.2 Hz, CH_3), 1.17 (dd, 3H, J = 15.6, 7.0 Hz, CH_3, *i*-Pr), 1.08 (dd, 3H, J = 16.0, 7.0 Hz, CH_3, *i*-Pr). ^{13}C NMR ($CDCl_3$, 126 MHz): δ 133.3 (s, C_{arom}), 133.1 (d, J = 12.9 Hz, C_{arom}), 128.1 (d, J = 8.9 Hz, C_{arom}), 128.0 (d, J = 8.9 Hz, C_{arom}), 28.4 (d, J = 18.1 Hz, CH_3), 18.5 (d, J = 5.4 Hz, CH, *i*-Pr), 7.6 (d, J = 17 Hz, CH_3, *i*-Pr), 7.5 (d, J = 16.3 Hz, CH_3, *i*-Pr). ^{31}P NMR ($CDCl_3$, 202 MHz): δ −24.0. HRMS calcd for $C_{40}H_{60}Cu_4I_4P_4$: $[M - I]^+$ = 1296.79581. Found: 1296.80912. Anal. calcd for $C_{40}H_{60}Cu_4I_4P_4$ (1426.61): C, 33.68; H, 4.24. Found: C, 33.67; H, 4.08. White crystals suitable for X-ray diffraction were obtained by slow diffusion of methanol in dichloromethane.

The enantiomeric complex (S_p)-**7** was prepared using a similar procedure as for (R_p)-**7**, but starting from the phosphine (*S*)-**4**. The ^{1}H NMR spectrum is identical: ^{31}P NMR ($CDCl_3$, 202 MHz): δ −24.8.

*Tetrameric[iodoheptadecylphenyl-i-propylphosphine)copper(I)]-(R_P)-**8**.* In a 50 mL two-necked flask equipped with a magnetic stirrer and an argon inlet, 0.39 g of phosphine (*R*)-**6** (1 mmol) and 0.2 g of CuI (1 mmol) were dissolved in 5 mL of toluene. The reaction mixture was heated at 60 °C overnight (a white solid appears). The solid is filtered on Millipore and washed with toluene to remove the excess copper. The solvent is evaporated, and the residue was purified by column chromatography on silica gel using a mixture of 95:5 hexane/ethyl acetate as the eluent to obtain 0.36 g of a colorless oil. Yield: 62%. Colorless oil. $[\alpha]_D^{25}$ = −12.3 (c 0.8, $CHCl_3$). ^{1}H NMR ($CDCl_3$, 500 MHz): δ 7.75 (m, 2H, CH_{arom}), 7.31 (m, 3H, CH_{arom}), 2.14 (m, 1H, C*H*, *i*-Pr), 2.03−1.61 (m, 4H, CH_2), 1.25−1.14 (br.s, 31H, CH_3 and $C_{17}H_{35}$), 0.98 (dd, 3H, J = 15.6, 7.0 Hz, CH_3, *i*-Pr), 0.81 (t, 3H, J = 6.7 Hz, CH_3, $C_{17}H_{35}$). ^{13}C NMR ($CDCl_3$, 126 MHz): δ 133.9 (d, J = 12.9 Hz, C_{arom}), 131.9 (d, J = 25.3 Hz, CH_{arom}), 129.8 (br.s, CH_{arom}), 128.2 (d, J = 9.0 Hz, CH_{arom}), 32.0 (s, CH_2), 31.7 (d, J = 13.1 Hz, CH_2), 29.8 (s, CH_2), 29.7 (s, CH_2), 29.6 (s, CH_2), 29.3 (d, J = 32.7 Hz, CH_2), 28.1 (d, J = 18.7 Hz, CH), 24.8 (d, J = 3.7 Hz, CH_2), 24.1 (d, J = 16.8 Hz, CH), 22.7 (s, CH_2), 18.8 (d, J = 6.9 Hz, CH_3), 18.7 (d, J = 4.9 Hz, CH_3), 14.1 (s, CH_3). ^{31}P NMR ($CDCl_3$, 202 MHz): δ −12.7. HRMS calcd for $C_{104}H_{188}Cu_4I_4P_4$: $[M - I]^+$ = 2193.79741. Found: 2193.79031. Anal. calcd for $C_{104}H_{188}Cu_4I_4P_4$ (2324.33): C, 53.74; H, 8.15. Found: C, 53.44; H, 8.41.

The enantiomeric complex (S_p)-**8** was prepared using a similar procedure as for (R_p)-**8**, but starting from the phosphine (*S*)-**6**. The ^{1}H NMR spectrum is identical. ^{31}P NMR ($CDCl_3$, 202 MHz): δ −12.0.

Instruments. The NMR spectra (^{1}H, ^{13}C, and ^{31}P) were recorded on Bruker 500 Avance DRX, 300 Avance, or 600 Avance II MHz or Bruker Avance 400 MHz FT-NMR spectrometers at room temperature using tetramethylsilane as an internal standard for ^{1}H and ^{13}C nuclei or 85% H_3PO_4 as an external standard for the ^{31}P nucleus. Data are reported as s = singlet, d = doublet, t = triplet, q = quartet, m = multiplet, br.s = broad singlet, integration, coupling constant(s) in Hz. Melting points were measured on a Kofler bench melting point apparatus and are uncorrected. Optical rotation values were determined at 25 °C on a Perkin-Elmer 341 polarimeter, using a 10

dx.doi.org/10.1021/ic400498j | *Inorg. Chem.* 2013, 52, 7958−7967

Scheme 1. Synthesis of (*R*)-(−)-3 and (*R*)-6[a]

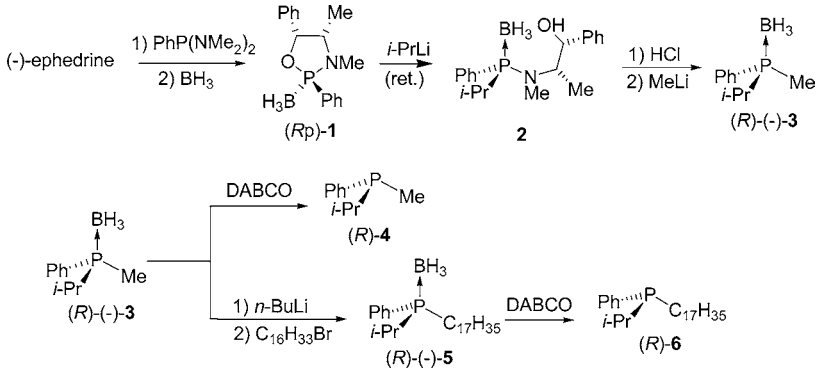

[a]Note that the syntheses of the (*S*)-analogues are the same.

cm quartz vessel. Mass spectral analyses were performed on a Bruker Daltonics microTOF-Q apparatus or on a Bruker AutoflexSpeed MALDI-TOF. The circular dichroism spectra were measured in dichloromethane on a JACSO J-810 spectropolarimeter. UV−visible spectra were obtained on an HP-8453 diode array spectrophotometer or on a Varian Cary 300 spectrophotometer. Emission and excitation spectra were measured on a Fluorolog 2 from SPEX or a LS100 from Photon Technology International (PTI). The emission lifetimes were measured on either an LS100 for phosphorescence or an N_2 laser system for fluorescence both from PTI. The N_2 source exhibited a fwhm ∼ 1400 ps, and the fluorescence lifetimes were obtained from deconvolution or distribution lifetimes analysis. The uncertainties were ∼50−100 ps. The phosphorescence lifetimes were measured using a 1 μs tungsten-flash lamp (fwhm ∼ 1 μs) and were also obtained from deconvolution.

Procedures. The quantum yield measurements using 9,10-diphenylanthracene as a standard were performed in methylcyclohexane at 298 K.[13] Three different measurements (i.e., different solutions) were prepared for each photophysical datum (quantum yields and lifetimes). The solutions for the samples and the reference were prepared under inert atmosphere in a glovebox. Solutions prepared for both the reference and the samples were adjusted to obtain absorbencies around 0.05 where three different solutions for each measurement were used. Each absorbance value was measured six times for better accuracy in the measurements of the quantum yields and was adjusted to be the same as much as possible for the standard and the sample for a measurement.

X-Ray Equipment and Refinement. Diffraction data were collected on a Nonius Kappa Apex II diffractometer equipped with a nitrogen jet stream low-temperature system (Oxford Cryosystems). The X-ray source was graphite monochromated Mo Kα radiation (= 0.71073 Å) from a sealed tube. The lattice parameters were obtained by least-squares fit to the optimized setting angles of the entire set of collected reflections. No significant intensity decay or temperature drift was observed during the data collections. Data were reduced by using HKL Denzo and Scalepack[14] software without applying absorption corrections, the missing absorption corrections were partially compensated by the data scaling procedure in the data reduction. The structure was solved by direct methods using the SIR92[15] program. Refinements were carried out by full-matrix least-squares on F^2, using the SHELXL-97[16] program on the complete set of reflections. Anisotropic thermal parameters were used for non-hydrogen atoms. All H atoms, on a carbon atom or oxygen atom, were placed at calculated positions using a riding model with C−H = 0.95 Å (aromatic), 0.99 Å (methylene), and 0.98 Å (methyl) with $U_{iso}(H) = 1.2U_{eq}(CH)$ or $U_{iso}(H) = 1.5U_{eq}(CH_3)$. Absolute configuration was determined reliably from anomalous scattering, using the Flack method.[17] A table and data are available in the Supporting Information.

X-Ray Powder Diffraction Patterns. The powder was mixed with Paratone Oil to obtain a paste like sample. This sample was cut to approximately 0.3 × 0.3 × 0.3 mm^3, placed on a needle and mounted on a Bruker APEX DUO X-ray diffractometer. Six correlated runs with a phi scan of 360° and exposure times of 360 s were collected with the Cu microfocus anode (1.54184 Å) and the CCD APEX II detector at a 150 mm distance. These runs, from −12 to −72 2-theta and 6 to 36 omega, were then treated and integrated with the XRW^2 Eval Bruker software to produce the X-ray powder diffraction patterns from 2.5 to 82° 2-theta. The pattern was treated with Diffrac.Eva version 2.0 from Bruker.

Small-Angle X-Ray Scattering. The SAXS patterns were collected with a Bruker AXS Nanostar system equipped with a microfocus copper anode at 45 kV/0.65 mA, MONTAL OPTICS, and a VANTEC 2000 2D detector at a 67.75 mm distance from the samples calibrated with a silver behenate standard. The solutions were prepared saturated in distilled THF and placed in quartz cells for measurements. The blanks were measured first and subtracted from the measured data. The diffracted intensities were then integrated from 0.15 to 5.00° 2-theta and treated with the Primus GNOM 3.0 program from ATSAS 2.3 software, to determine the particle sizes by pair distance distribution.[18]

Computer Modeling. These computations based on molecular mechanics (MMX) were performed using the commercially available package PCModel v.7.0 from Serena Software. No bond or angle was fixed.

RESULTS AND DISCUSSION

Ligand Synthesis. The stereoselective synthesis of the (*R*)- and the (*S*)-phosphine ligands **4** and **6** was performed in several steps using (−)- and (+)-ephedrine,[9f] respectively, where the precursors **1**−**3** are already known (Scheme 1).[12a] (*R*)-(−)- or (*S*)-(−)-methylphenyl-*i*-propylphosphine borane (**3**) reacts with *n*-BuLi to form the α-carbanion $LiCH_2P(BH_3)(Ph)(i\text{-}Pr)$, which reacts with the hexadecyl bromide $C_{16}H_{33}Br$ to afford the heptadecyl derivative **5** in 56% yield. Deprotection of **3** and **5** with DABCO leads to the corresponding free phosphines **4** and **6** in good to excellent yields (98%) and with e.e. up to 96%.

Scheme 2

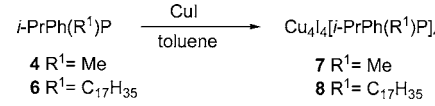

Synthesis and Characterization of the Copper Complexes. The complexes were prepared from both enantiomers of phosphines **4** and **6** by reacting them directly with CuI in toluene at 60 °C (Scheme 2). For the sake of

dx.doi.org/10.1021/ic400498j | Inorg. Chem. 2013, 52, 7958−7967

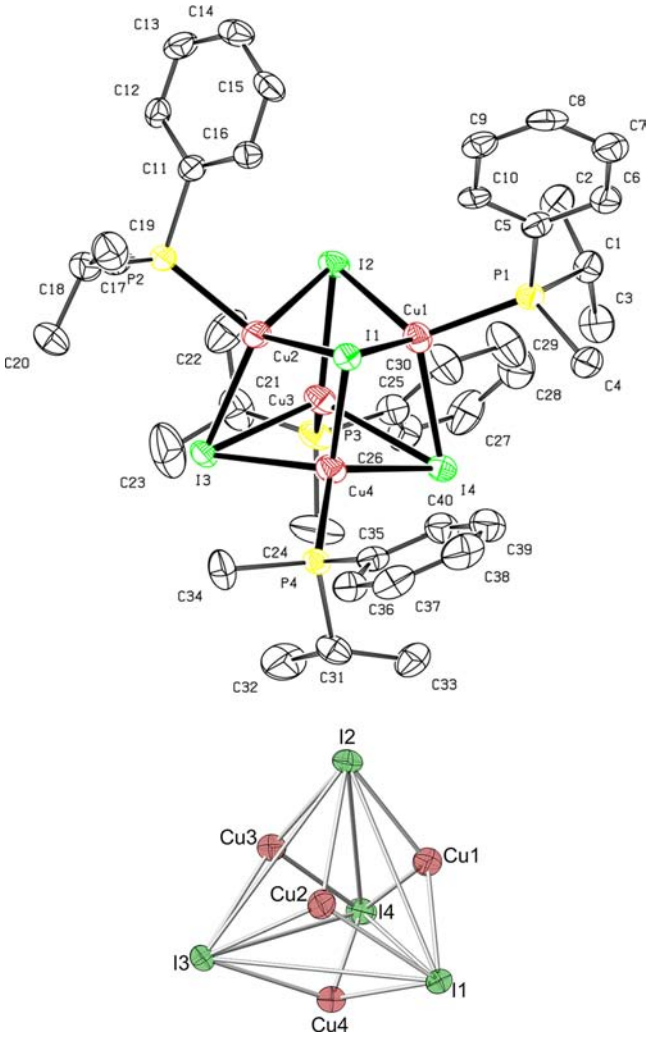

Figure 1. Top: ORTEP[19] view of compound (R_p)-**7**. Hydrogen atoms have been omitted for clarity. Bottom: Highlighting of triakis tetrahedron in compound (R_p)-**7**. Nonmetallic atoms have been omitted for clarity. The thermal ellipsoids at the 50% probability level for both representations.

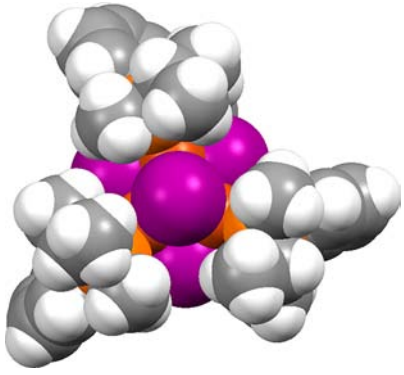

Figure 2. Space filling model of (R_p)-**7** showing the pseudo (or local) C_3 axis (I = purple; Cu = dark orange; P = light orange). Note that the fourth phosphine ligand behind the cluster is not considered.

simplicity, the nomenclature of the copper complexes **7** (or **8**) prepared from the phosphine (*S*)- or (*R*)-**4** (or **6**) are called (S_p)-**7** or (R_p)-**7** (or (S_p)-**8** or (R_p)-**8**), respectively,

Table 1. Selected Bond Lengths (Å) for Compound (R_p)-7

Cu(1)−Cu(2)	2.9573(13)	Cu(1)−I(1)	2.7052(10)
Cu(1)−Cu(3)	2.8797(13)	Cu(1)−I(2)	2.6324(10)
Cu(2)−Cu(3)	2.8808(14)	Cu(1)−I(4)	2.7439(11)
Cu(2)−Cu(4)	2.9522(13)	Cu(2)−I(1)	2.6085(10)
Cu(3)−Cu(4)	2.9791(13)	Cu(2)−I(2)	2.7976(11)
Cu(1)−Cu(4)	3.0736(13)	Cu(2)−I(3)	2.7014(10)
		Cu(3)−I(2)	2.6547(11)
		Cu(3)−I(3)	2.6923(10)
		Cu(3)−I(4)	2.7445(11)
		Cu(4)−I(1)	2.7253(11)
		Cu(4)−I(3)	2.7103(10)
		Cu(4)−I(4)	2.6375(11)

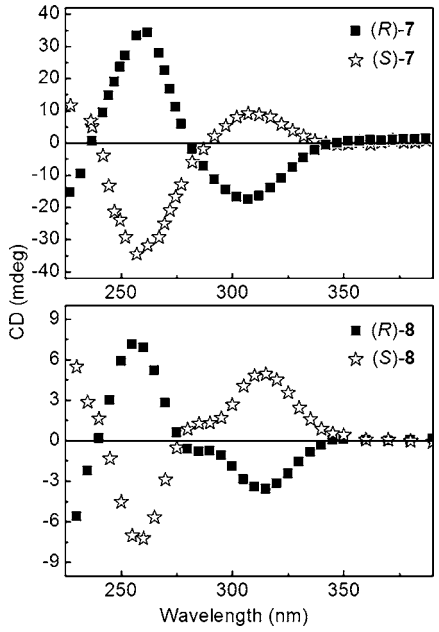

Figure 3. CD spectra of (R_p)-**7**, (S_p)-**7**, (R_p)-**8**, and (S_p)-**8** in CH_2Cl_2 at 298 K. The θ [deg cm^2 dmol^{-1}] data are provided in Table S5 for convenience.

independently of the absolute configuration of the phosphorus centers in the complexes.

Clusters (S_p)-**8** or (R_p)-**8** are oily materials at room temperature. So no crystal was obtained for these species. Conversely, colorless prismatic chiral crystals were obtained by slow evaporation of (R_p)-**7** in a dichloromethane/methanol mixture. Single crystal X-ray analysis showed that this compound contains a triakis tetrahedron of copper atoms, with facially capping iodides (Figure 1), and chirality is apparent from the presence of a pseudo-C_3 axis formed by three of the phosphine ligands (Figure 2).

Bond lengths of the "Cu_4I_4" skeleton are presented in Table 1 and are found to be normal in comparison with distances reported for other cubane complexes containing the $Cu_4I_4P_4$ frame. More specifically, the Cu···Cu and Cu···I distances range from 2.8797(13) to 3.0736(13) Å, averaging 2.954 Å, and from 2.6085(10) to 2.7976(11) Å, averaging 2.696 Å, respectively. Although these average distances fall substantially short comparatively to those observed for $Cu_4I_4(t\text{-}Bu_3P)_4$ (Cu···Cu: 3.560 and Cu···I: 2.731 Å),[20] $Cu_4I_4(P(C_7H_8)_3)_4$ (Cu···Cu: 3.247 and Cu···I: 2.713 Å),[21] and $Cu_4I_4(P(NH_2)_3)_4$ (Cu···Cu: 3.386 and Cu···I: 2.726 Å),[22] these distances compare more

dx.doi.org/10.1021/ic400498j | Inorg. Chem. 2013, 52, 7958−7967

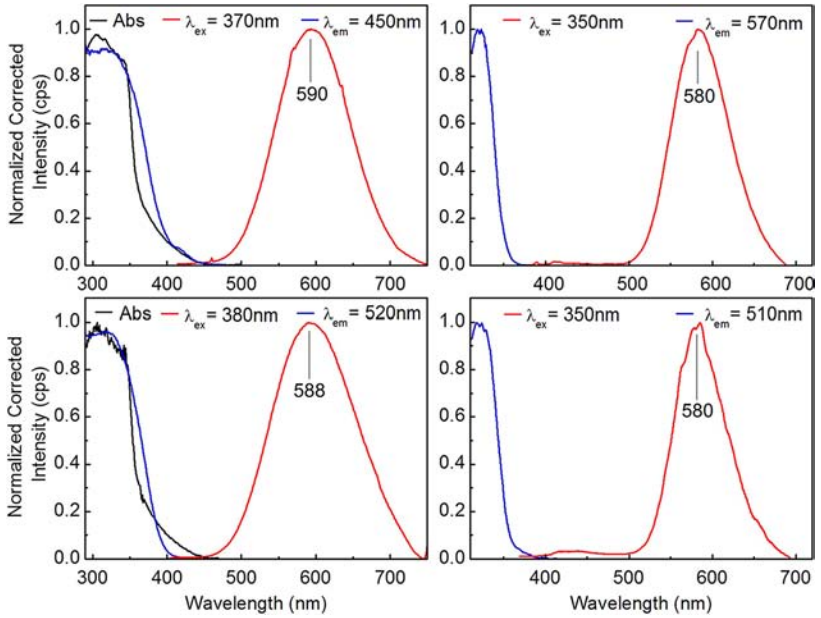

Figure 4. Absorption (black), excitation (blue), and emission (red) spectra of (R_p)-7 (top) and (S_p)-7 (bottom) at 298 K (left) and 77 K (right) in the solid state. The uncertainty on the maxima is ±5 nm.

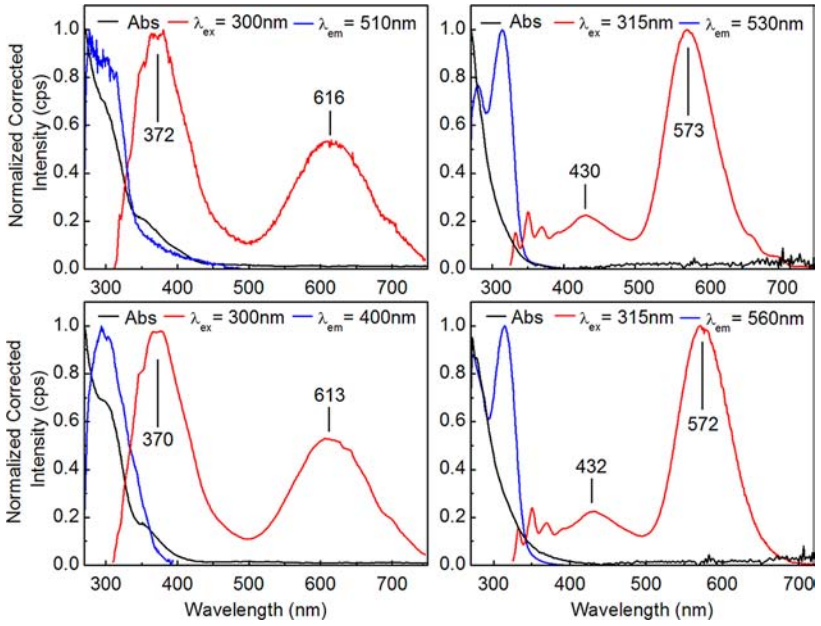

Figure 5. Absorption (black), excitation (blue), and emission (red) spectra of (R_p)-7 (top) and (S_p)-7 (bottom) at 298 K (left) and 77 K (right) in methylcyclohexane. The uncertainty on the maxima is ±5 nm.

favorably to those reported for $Cu_4I_4(P(C_6H_5)_2CH_3)_4$ (Cu···Cu: 2.930 and Cu···I: 2.705 Å),[23] $Cu_4I_4(P(C_6H_5)_3)_4$ (Cu···Cu: 2.968 and Cu···I: 2.693 Å),[24] $Cu_4I_4(P(C_6H_5CH_3)_3)_4$ (Cu···Cu: 3.023 and Cu···I: 2.680 Å),[25] $Cu_4I_4(P(C_6H_5)_2Fc)_4$ (Fc = ferrocenyl, Cu···Cu: 3.071, and Cu···I: 2.692 Å),[26] $Cu_4I_4(P(C_6H_5)_2C_3H_7)_4$ (Cu···Cu: 3.143 and Cu···I: 2.690 Å),[27] and $Cu_4I_4(P(C_6H_{11})_3)_4$ (Cu···Cu: 3.142 and Cu···I: 2.692 Å).[10i] Three cubanes exhibiting the smallest Cu···Cu and Cu···I distances are those for the recently reported structures of $Cu_4I_4(P(C_6H_5)_3)_4$ (Cu···Cu: 2.873 and Cu···I: 2.681 Å)[11e] and $Cu_4I_4(P(C_6H_5)_3$(pyrimidine-2,4(1H,3H)-dione-P))$_4$ (Cu···Cu: 2.885 and Cu···I: 2.677 Å).[10] X-ray powder diffraction spectroscopy was used to confirm that both (R_p)-7 and (S_p)-7 isomers are the enantiomers of each other. Indeed, the calculated pattern for (R_p)-7 from the X-ray structure was almost identical to that measured for (S_p)-7 (Figure S17).

Because of the presence of long chains on (S_p)-**8** and (R_p)-**8** and their very viscous behavior, one of them, (S_p)-**8**, was further investigated under a polarized microscope searching for a mesophase. No birefringence activity was observed with polarized light under a microscope all the way down to −10 °C, even after several hours. Small-angle X-ray scattering patterns were also measured (Figure S18). A weak and broad scattering was observed at ∼2.8° (2θ) in silicone matrices, indicating the presence of organization. Assuming that most of the scattered X-rays arise from the heavy elements (i.e., Cu_4I_4), the intercluster distance, d, is found to be 31.6 Å. Assuming full side-by-side $C_{17}H_{35}\cdots C_{17}H_{35}$ contacts, computer modeling

dx.doi.org/10.1021/ic400498j | Inorg. Chem. 2013, 52, 7958−7967

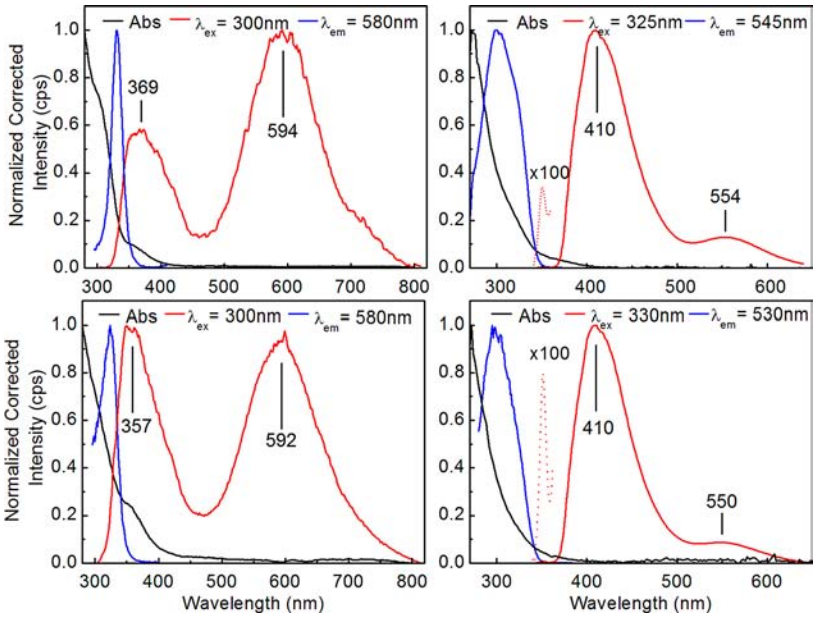

Figure 6. Absorption (black), excitation (blue), and emission (red) spectra of (R_p)-**8** (top) and (S_p)-**8** (bottom) at 298 (left) and 77 K (right) in methylcyclohexane. The uncertainty on the maxima is ±5 nm.

Table 2. Spectroscopic Data for the Chiral Clusters in the Solid State or in Methylcyclohexane

		298 K			77 K		
		λ_{abs} (nm)	λ_{emi} (nm)	Δ (cm^{-1})[a]	λ_{abs} (nm)[b]	λ_{emi} (nm)	Δ (cm^{-1})[a]
(R_p)-7	solid state	336	590	12800	315	580	14500
(S_p)-7	solid state	336	588	12800	315	580[c]	14500
(R_p)-7	solution	298	372	6700	314	430	8600
			616	17300		573	14400
(S_p)-7	solution	298	370	6500	315	432	8600
			615	17300		572	14500
(R_p)-**8**	solution	321[b]	369	4000	307	410	8200
			594	14300		554	14500
(S_p)-**8**	solution	300[b]	357	5300	299	410	9000
			592	16400		550	15300

[a] Δ(cm^{-1}) = ($10^7/\lambda_{abs}$ (nm)) − ($10^7/\lambda_{emi}$ (nm)); i.e. Stokes shift in cm^{-1}, a linear scale of energy. [b] The position of the maximum is extracted from the excitation spectra. [c] A weak signal is also noted at ~425 nm.

indicates that the average (S_p)-**8** cluster/(S_p)-**8** cluster distance is ~29.2 Å (Figure S19). In conclusion, the clusters **8** in the pure state exhibit some structural organization that greatly depends on the presence of alkyl chains. Because of the tetrahedral geometry of the cluster, the formation of a gel is not excluded.

Finally, the circular dichroism (CD) spectra of (R_p)-**7**, (S_p)-**7**, (R_p)-**8**, and (S_p)-**8** in CD_2Cl_2 exhibit the expected mirror image relationship of each other (Figure 3), confirming their relative chirality. Their polarized activities occur in the 220−350 nm range in line with the position of their absorption spectra below (Figures 4−6).

Electronic and Luminescence Spectra. These absorption and emission spectra of the strongly emissive (R_p)-**7**, (S_p)-**7**, (R_p)-**8**, and (S_p)-**8** clusters in the solid state and in solution (methylcyclohexane as noncoordinating solvent) are shown in Figures 4−6, and a picture of a glowing solid sample is placed in the Supporting Information (Figure S20). The spectra for the (*R*)- and (*S*)-enantiomers are essentially identical as expected, and the band maxima in the absorption, excitation (when appropriate), emission spectra, and Stokes shifts (Δ(cm^{-1})) are placed in Table 2.

The absorption spectra exhibit features at wavelengths shorter than 400 nm, consistent with the off white coloration of the solid (**7**) and liquid (**8**), and resemble those reported by Perruchas and co-workers.[11c] The emission spectra, for most cases, consist of the characteristic double emission, i.e. two bands, one in the range of ~400−500 and the other in the ~500−700 nm window known for $Cu_4I_4P_4$ cubanes[11] and other $Cu_4I_4L_4$-containing materials (L = pyridine[28] or mono- and dithioethers,[29] for examples). These two emissions are characterized by Stokes shifts of 4000−9000 and of 12 800−17 300 cm^{-1} for the high- and low-energy emissions, respectively. The large Stokes shifts and the microsecond time scales of their lifetimes (placed below) indicate phosphorescence. The relative intensity of the two bands changes drastically for these species in solutions going from 298 down to 77 K, which is reminiscent of the known thermochromic behavior of several $Cu_4I_4P_4$ cubanes.[11b−f] The assignment of the two excited states involved in these two emissions was previously investigated by different research groups. Indeed, Ford and collaborators addressed this problem in the 1990s using ab initio calculations,[30] and more recently using density functional theory (DFT).[31] The main conclusion is that these two excited states are either cluster centered (CC*, i.e within the Cu_4X_4 skeleton) or halide-to-ligand charge transfer (XLCT). The recent calculations reported by Vega and Saillard also agreed with these conclusions.[10e] More recently, Perruchas and co-workers also used DFT to address the nature of low and high energy emission bands and came to a similar conclusion with a slight modification. The low energy emission ($T_1 \rightarrow S_0$) is assigned to a combination of a halide-to-copper charge transfer transition (XMCT) and a copper-centered transition (3d→4s, 4p, i.e., CC*), which is essentially independent of the nature of the ligand. The high energy emission ($T_2 \rightarrow S_0$) corresponds to a ^{3}XLCT/^{3}MLCT mixed

dx.doi.org/10.1021/ic400498j | Inorg. Chem. 2013, 52, 7958−7967

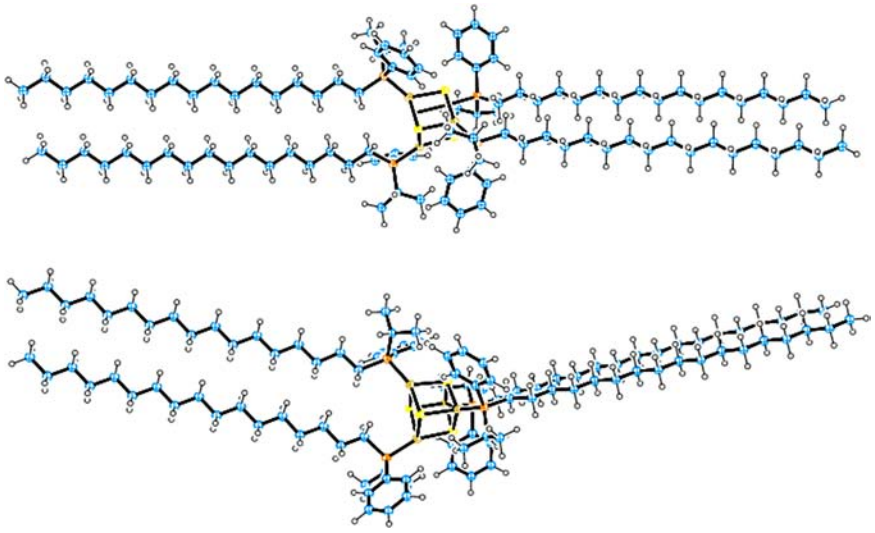

Figure 7. Top and side views of a computer model (*vide infra*) of (S_p)-**8** stressing on the possible $C_{17}H_{35}$ chain autoassembly.

Table 3. Fluorescence and Phosphorescence Quantum Yields Measured Methylcyclohexane at 298 K[a]

compound	Φ_F ($\times 10^{-2}$)	Φ_P ($\times 10^{-2}$)
(R_p)-7	28.6	8.7
(S_p)-7	28.6	8.7
(R_p)-**8**	8.9	6.3
(S_p)-**8**	8.9	6.3

[a]The uncertainties are ±10%.

transition.[11c] On the basis of the similitude in Cu···Cu (2.954) and Cu···I (2.696 Å) distances for (R_p)-7 with that of $Cu_4I_4(P(C_6H_5)_3)_4$ used by Perruchas and co-workers (2.9012(6) and 2.6838(5) Å),[11c] the nature of these emissions are reasonably assumed to be the same: ^{3}XLCT/^{3}MLCT ($T_2 \rightarrow S_0$) and ^{3}CC ($T_1 \rightarrow S_0$).

Interestingly, the low energy emission is profoundly more intense for (R_p)-7 and (S_p)-7 in the solid state at both 298 and 77 K (Figure 4). However, the relative intensity ratio of the high energy band/low energy band becomes larger when (R_p)-7 and (S_p)-7 are in solution (2-methylcyclohexane; Figure 5), again at both temperatures, in comparison with the solid state spectra. This behavior strongly suggests that the rigidity of the medium plays a role in this property, where the solid state is more rigid than both fluid and frozen solutions.

One very interesting observation is the striking difference in relative intensity ratio of the high energy band/low energy band between (R_p)-7 and (S_p)-7 vs (R_p)-**8** and (S_p)-**8** (Figures 5 and 6). The clusters exhibit essentially opposite trends in these relative emission intensities at both temperatures. The role of the long chains in the temperature dependence of the relative intensity of these two emissions remains unknown, although computer modeling suggests that the $C_{17}H_{35}$ chains can autoassemble by pairs (Figure 7). Finally, weak and structured emissions are depicted in the vicinity of 350 nm. This feature is believed to be associated with an intraligand (C_6H_5P) $\pi\pi^*$ emission, likely fluorescence due to the spectral proximity to the absorption. This assignment is supported by the detection of a nanosecond lifetime decay at this wavelength (see below). The quantum yield data, Φ, at 298 K are placed in Table 3.

The emission lifetimes, τ_e, for these two emissions range from 5 to 200 μs (Table 4) and compare favorably to that reported for other $Cu_4I_4L_4$-containing materials (for example L = pyridine[28] or mono- and dithioether),[29,32] including those which contain phosphine ligands (details are provided in Table S6 for convenience, SI). As previously stated above, the microsecond time scale also indicates that these emissions arise from triplet manifolds so that these are better referred to as phosphorescence (i.e., their lifetimes are noted as τ_P). Several other features are noted. First, the τ_P values are expectedly

Table 4. Fluorescence and Phosphorescence Lifetimes As Solid or in Methylcyclohexane (MCH)[a]

	298 K		77 K	
compd.	τ_F (ns)	τ_P (μs)	τ_F (ns)	τ_P (μs)
(R_p)-7 solid state		5.2 ± 0.1 (590)		13.1 ± 0.1 (585)
(S_p)-7 solid state		5.2 ± 0.1 (590)		13.1 ± 0.1 (575)
(R_p)-7 in MCH	4.5 ± 0.2 (350)	9.2 ± 0.1 (375)	15.5 ± 0.6 (350)	119.0 ± 0.4 (430)
		13.0 ± 0.1 (620)		107.0 ± 0.1 (585)
(S_p)-7 in MCH	4.6 ± 0.4 (350)	9.2 ± 0.1 (375)	15.3 ± 0.2 (350)	119.0 ± 0.5 (430)
		12.7 ± 0.1 (620)		106.8 ± 0.2 (585)
(R_p)-**8** in MCH	4.7 ± 0.4 (350)	13.7 ± 0.1 (360)	21.9 ± 0.2 (350)	193.0 ± 0.1 (415)
		12.8 ± 0.1 (595)		39.8 ± 0.3 (560)
(S_p)-**8** in MCH	4.9 ± 0.6 (350)	13.4 ± 0.01 (360)	21.5 ± 0.4 (350)	193.0 ± 0.8 (415)
		12.9 ± 0.1 (595)		39.4 ± 0.1 (560)

[a]The values in parentheses are the emission maxima also where the measurements were performed.

dx.doi.org/10.1021/ic400498j | *Inorg. Chem.* 2013, 52, 7958−7967

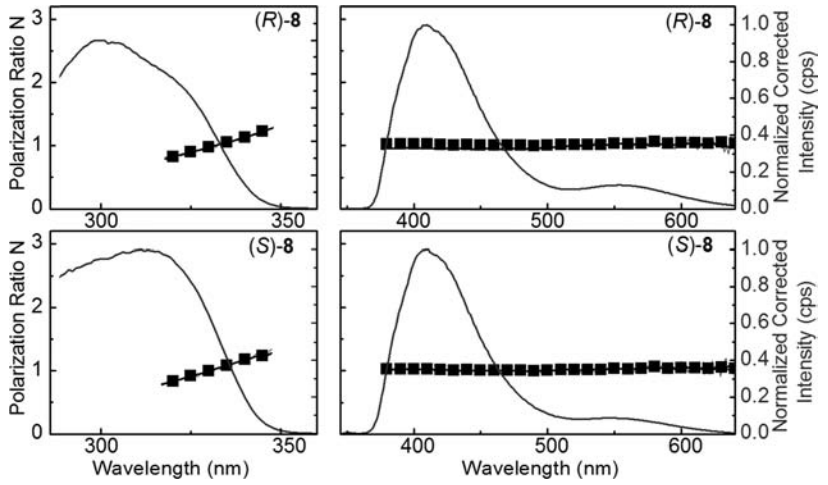

Figure 8. Polarization ratios of the excitation (left; λ_{em} = 420 nm) and emission (right; λ_{exc} = 330 nm) spectra of (R_p)-**8** and (S_p)-**8** in methylcyclohexane at 77 K. The *N* values approaching and below 300 and exceeding 350 nm are uncertain due to weak instrument response and a weak signal, respectively. The uncertainties on the measurements are ±0.2.

identical (within the uncertainties) for both enantiomers. Second, τ_P increases upon cooling the temperature for all cases, which is consistent with the increase in medium rigidity. Third, the τ_P values increase upon going from the solid state to the solution, suggesting that intermolecular proximity induces more nonradiative excited state deactivation processes. This could also explain the very low intensity or absence of the high energy band. Fourth, the weak structured emission appearing in the vicinity of 350 nm exhibits decays on the nanosecond time scale (4−5 ns, 298 K; 15−22 ns, 77 K), which is fully consistent with the intraligand (C_6H_5P-) $\pi\pi^*$ fluorescence assignment. Finally, the τ_P values of the high and low energy emissions are similar (in solution) for all cases except that for (R_p)-**8** and (S_p)-**8** at 77 K, for which these lifetimes are significantly shorter for the low energy band in comparison with the high one, which is consistent with the much weaker intensity.

The polarization ratios, *N*, of both the emission and excitation spectra were measured using the photoselection method.[33] The *N* values are obtained from $N = (I_{\parallel} \times I_{\perp})_{\parallel}/(I_{\parallel} \times I_{\perp})_{\perp}$, where $I_{\parallel}$ and $I_{\perp}$ are the emission intensity when the polarizers are placed parallel and perpendicular to each other with the excitation polarizer placed either parallel or perpendicular to the floor for $(I_{\parallel} \times I_{\perp})_{\parallel}$ and $(I_{\parallel} \times I_{\perp})_{\perp}$, respectively. With molecules rigidly held in frozen solutions, the relative orientations of the transition moments are randomly distributed, and the *N* values may have maximum and minimum theoretical values of 3.0 and 0.5, respectively. The former and latter values indicate that the emitted light is respectively polarized parallel and perpendicular with respect to the transition moment of the absorption. For the case where *N* = 1, the emitted light is polarized along the three Cartesian axes.

In the case of emissions arising from triplet states, the probability for the radiative transitions, *P*, is given by $P = \int \Phi_e\Phi_s\Phi_v|\mu_e|\Phi_e'\Phi_s'\Phi_v'\, d\tau$ where Φ_e and Φ_e', Φ_s and Φ_s', and Φ_v and Φ_v' are respectively the electronic, spin, and vibrational wave functions of the starting and arriving states, and μ_e is the transition moment operator. This expression can be treated using the group theory where the product of all these terms must give an answer that contains the totally symmetric term. Assuming that an approximate T_d symmetry can be applied (i.e., $T_1 \rightarrow S_0$; $a_1 \rightarrow t_2$),[11c] then the symmetry of the low energy ^{3}CC emissive state is $\Phi_e = {}^3T_2$ and $\Phi_s = R_{x,y,z}$ (*R* is for rotation or spin; i.e. t_1) whereas the diamagnetic ground state is $\Phi_e' = {}^1A_1$ but also $\Phi_s' = a_1$. Assuming that the cluster sits on the lowest energy vibrational level $v = 0$, then Φ_v and Φ_v' are totally symmetric (i.e., a_1). With $\mu_e = T_{x,y,z}$ (*T* is for transition moment or translation; here t_2), the product of the seven terms is, in the same order as above, $P = T_2 \times t_1 \times a_1 \times t_2 \times A_1 \times a_1 \times a_1$. The product $T_2 \times t_1(R_{x,y,z})$ gives $a_1 + e + t_1 + t_2$, and then the product $(a_1 + e + t_1 + t_2) \times t_2$ includes the operation $t_2 \times t_2 = (t_2)^2$, which gives an answer that contains the totally symmetric term a_1. Note that the product of any term by a_1 gives this same term. The conclusion of this analysis is that this spin forbidden radiative process $^3T_2 \rightarrow {}^1A_1$ occurs with a low probability with a transition moment polarized along the *x*, *y*, and *z* axes (i.e., t_2). Consequently, *N* is bound by symmetry to be 1 for the pure electronic transitions. This theoretical prediction is indeed experimentally verified for the (R_p)-**8** and (S_p)-**8**. Noteworthy is that both ^{3}XLCT/LXCT ($T_2 \rightarrow S_0$) and ^{3}CC ($T_1 \rightarrow S_0$) emissions exhibit *N* = 1 (Figure 8).

Final Comments. Copper complexes of the general formula $[Cu_4I_4L_4]$ (L = P-chirogenic ligand) have been synthesized from the very convenient (−)- and (+)-ephedrine methodology providing species with e.e. up to 96%. The clusters were fully characterized, including X-ray structure, X-ray diffraction patterns, and CD spectra. For further applications, it is also reasonable to suspect that the chiral induction for reactions utilizing the (*R*)-**6** and (*S*)-**6** ligands (with $C_{17}H_{35}$) will be different with respect to those using (*R*)-**4** and (*S*)-**4** (with CH_3) based on a simple steric argument. Moreover, the electronic spectral signatures and photophysical properties arising from the $Cu_4I_4P_4$ core clearly demonstrate the close similarity with those for the few achiral analogues reported so far. One particularity is the presence of the long $C_{17}H_{35}$ chains that influences the photophysical parameters (i.e., decrease of Φ_P and τ_P upon cooling) with respect to those for CH_3. Autoassembling of the $C_{17}H_{35}$ long chains (i.e., pairing) may most likely occur at lower temperatures. This would be in line with the SAXS findings. If verified, then the design of nematic liquid crystals may also be possible by finding the appropriate substituents to be placed on the phosphorus atom, but with the particularity that they contain a thermochromic luminescent core. Moreover, preliminary results on the catalytic addition of

dx.doi.org/10.1021/ic400498j | Inorg. Chem. 2013, 52, 7958−7967

phenylmagnesium bromide on cyclohex-2-enone give the racemic adduct phenyl-3-cyclohexanone in 81% conversion after one hour using both (R_p)-**7** and (R_p)-**8** as a catalyst (SI). Despite these modest preliminary results, further works are in progress to improve the enantioselectivity of this reaction using functional P-chirogenic phosphines.

■ ASSOCIATED CONTENT

Supporting Information

X-ray crystallographic structure of (R_p)-**7** in CIF format. ^{1}H, ^{13}C, and ^{31}P NMR spectra of (*R*)- and (*S*)-**4**, (*R*)-**5**, (**R**)-**6**, and cluster **8** prepared from (*R*)- and (*S*)-**6**. Photography of (R_p)-**7** under natural light (left) and UV lamp 254 nm (right). CD data for chiral compounds **7** and **8**. X-ray powder spectra for (S_p)-**7** and calculated for (R_p)-**7**. Log plot of the SAXS traces of cluster (S_p)-**8** in silicone compared to silicone. Molecular modeling of two (S_p)-**8** clusters interacting via $C_{17}H_{35}\cdots C_{17}H_{35}$ contacts. General procedure for the conjugate addition of phenylmagnesium bromide with cyclohex-2-enone **9**, in presence of copper(I) complexes (R_p)-**7** or (R_p)-**8**. This material is available free of charge via the Internet at http://pubs.acs.org.

■ AUTHOR INFORMATION

Corresponding Author

*Tel.: 1-819-821-7092 (P.D.H.), +33(0)3 80 39 61 13 (S.J.). E-mail: Pierre.Harvey@USherbrooke (P.D.H.), Sylvain.Juge@u-bourgogne.fr (S.J.).

Notes

The authors declare no competing financial interest.

■ ACKNOWLEDGMENTS

This research was supported by the Natural Sciences and Engineering Research Council of Canada (NSERC), le Fonds Québécois de la Recherche sur la Nature et les Technologies (FQRNT), the Centre d'Etudes des Matériaux Optiques et Photoniques de l'Université de Sherbrooke (CEMOPUS), and l'Agence Nationale de la Recherche (France) for the grant *MetChirPhos* and the Award of a Research chair of Excellence to P.D.H. We thank Dr. Pierre Lavigne (Faculté de Médecine of the Université de Sherbrooke) for letting us use his circular dichroism spectrometer, and Dr. J. Bayardon for helpful discussion and his help in the preparation of this manuscript.

■ REFERENCES

(1) (a) Beletskaya, I. P.; Cheprakov, A. V. *Coord. Chem. Rev.* **2004**, *248*, 2337−2364. (b) Liu, Y.; Wan, J.-P. *Org. Biomol. Chem.* **2011**, *9*, 6873−6894. (c) Deutsch, C.; Krause, N.; Lipshultz, B. H. *Chem. Rev.* **2008**, *108*, 2916−2927. (d) Yamada, K.-i.; Tomioka, K. *Chem. Rev.* **2008**, *108*, 2874−2886. (e) Reymond, S.; Cossy, J. *Chem. Rev.* **2008**, *108*, 5359−5406. (f) Monnier, F.; Taillefer, M. *Angew. Chem., Int. Ed.* **2008**, *47*, 3096−3099. (g) Kaddouri, H.; Vicente, V.; Ouali, A.; Ouazzani, F.; Taillefer, M. *Angew. Chem., Int. Ed.* **2009**, *48*, 333−336.

(2) Ranu, B. C.; Dey, R.; Chatterjee, T.; Ahammed, S. *ChemSusChem* **2012**, *5*, 22−44.

(3) (a) Alexakis, A.; Bäckvall, J. E.; Krause, N.; Pàmies, O.; Diéguez, M. *Chem. Rev.* **2008**, *108*, 2796−2823. (b) Stanley, L. M.; Sibi, M. P. *Chem. Rev.* **2008**, *108*, 2887−2902.

(4) (a) Knochel, P.; Yang, X.; Commermann, N. Polyfunctional 1,1-Organodimetallic for Organic Synthesis. In *Handbook of Functionalized Organometallics*; Knochel, P., Ed.; Wiley-VCH: Weinheim, Germany, 2005; Vol. 2. (b) Thaler, T.; Knochel, P. *Angew. Chem., Int. Ed.* **2009**, *48*, 645−648.

(5) (a) Tang, W.; Zang, X. *Chem. Rev.* **2005**, *103*, 3029−3069. (b) Jacobsen, E. N.; Pfaltz, A.; Yamamoto, H. *Comprehensive Asymmetric Catalysis*; Springer: New York, 2004. (c) Shimidzu, H.; Nagasaki, I.; Saito, T. *Tetrahedron* **2005**, *61*, 5405−5432. (d) Arrayas, R. G.; Adrio, J.; Carretero, J. C. *Angew. Chem., Int. Ed.* **2006**, *45*, 7674−7715. (e) Hargaden, G. C.; Guiry, P. J. *Chem. Rev.* **2009**, *109*, 2505−2550.

(6) (a) Borner, A. *Phosphorous Ligands in Asymmetric Catalysis*; Wiley-VCH: Weinheim, Germany, 2008; Vol. 3. (b) *Phosphorus (III) Ligands in Homogeneous Catalysis: Design and Synthesis*; Kamer, P. C. J., van Leeuwen, P. W. N. M., Eds.; Wiley: New York, 2012.

(7) (a) Yamanoi, Y.; Imamoto, T. *J. Org. Chem.* **1999**, *64*, 2988−2989. (b) Ito, H.; Ito, S.; Matsuura, K.; Sawamura, M. *J. Am. Chem. Soc.* **2007**, *129*, 14856−14857.

(8) (a) Pietrusiewicz, K. M.; Zablocka, M. *Chem. Rev.* **1994**, *94*, 1375−1411. (b) Kolodiazhnyi, O. I. *Tetrahedron: Asymmetry* **1998**, *9*, 1279−1332. (c) Ohff, M.; Holz, J.; Quirmbach, M.; Börner, A. *Synthesis* **1998**, 1391−1415. (d) Crépy, K. V. L.; Imamoto, T. *Top. Curr. Chem.* **2003**, *229*, 1−40. (e) Berthod, M.; Mignani, G.; Woodward, G.; Lemaire, M. *Chem. Rev.* **2005**, *105*, 1801−1836. (f) Grabulosa, A.; Granell, J.; Muller, G. *Coord. Chem. Rev.* **2007**, *251*, 25−90. (g) Imamoto, T. J. *Synth. Org. Chem., Jpn.* **2007**, *65*, 1060−1069. (h) Bayardon, J.; Laureano, H.; Diemer, V.; Dutartre, M.; Das, U.; Rousselin, Y.; Henry, J.-C.; Colobert, F.; Leroux, F. R.; Jugé, S. *J. Org. Chem.* **2012**, *77*, 5759−5769.

(9) (a) Nagel, U.; Rieger, B. *Organometallics* **1989**, *8*, 1534−1538. (b) Nagel, U.; Roller, C. *Z. Naturforsch. B: Chem. Sci.* **1998**, *53*, 267−270. (c) Moulin, D.; Darcel, C.; Jugé, S. *Tetrahedron: Asymmetry* **1999**, *10*, 4729−4743. (d) Darcel, C.; Moulin, D.; Henry, J. C.; Lagrelette, M.; Richard, P.; Harvey, P. D.; Jugé, S. *Eur. J. Org. Chem.* **2007**, *13*, 2078−2090. (e) Khiri, N.; Bertrand, E.; Ondel-Eymin, M.-J.; Rousselin, Y.; Bayardon, J.; Harvey, P. D.; Jugé, S. *Organometallics* **2010**, *29*, 3622−3631. (f) Lapprand, A.; Khiri, N.; Fortin, D.; Jugé, S.; Pierre, D.; Harvey, P. D. *Inorg. Chem.* **2013**, *52*, 2361−2371.

(10) (a) Churchill, M. R.; Kalra, K. L. *Inorg. Chem.* **1974**, *13*, 1899−1904. (b) Attar, S.; Bowmaker, G. A.; Alcock, N. W.; Frye, J. S.; Bearden, W. H.; Nelson, J. H. *Inorg. Chem.* **1991**, *30*, 4743−4753. (c) Cole, J. R.; Dellinger, M. E.; Johnson, T. J.; Reinecke, B. A.; Pike, R. D.; Pennington, W. T.; Krawiec, M.; Rheingold, A. L. *J. Chem. Cryst.* **2003**, *33*, 341−347. (d) Li, Y.; Yung, K.-F.; Chan, H.-S.; Wong, W.-T. *Inorg. Chem. Commun.* **2003**, *6*, 1451−1453. (e) Vega, A.; Saillard, J. Y. *Inorg. Chem.* **2004**, *43*, 4012−4018. (f) Seddigi, Z. S.; Hossain, G. M. G.; Banu, A. *Acta Crystallogr.* **2007**, *E63*, m756−m758. (g) Altaf, M.; Stoeckli-Evans, H. *Inorg. Chim. Acta* **2010**, *363*, 2567−2573. (h) Deng, S.; Schwarzmaier, C.; Zabel, M.; Nixon, J. F.; Bodensteiner, M.; Peresypkina, E. V.; Balazs, G.; Scheer, M. *Eur. J. Inorg. Chem.* **2011**, 2991−3001. (i) Nixon, T. D.; Gamble, A. J.; Thatcher, R. J.; Whitwood, A. C.; Lynam, J. M. *Inorg. Chim. Acta* **2012**, *380*, 252−260.

(11) (a) Lai, D. C.; Zink, J. I. *Inorg. Chem.* **1993**, *32*, 2594−2596. (b) Perruchas, S.; Le Goff, X. F.; Maron, S.; Maurin, I.; Guillen, F.; Garcia, A.; Gacoin, T.; Boilot, J. P. *J. Am. Chem. Soc.* **2010**, *132*, 10967−10969. (c) Perruchas, S.; Tard, C.; Le Goff, X. F.; Fargues, A.; Garcia, A.; Khalal, S.; Saillard, J. Y.; Gacoin, T.; Boilot, J. P. *Inorg. Chem.* **2011**, *50*, 10682−10692. (d) Maini, L.; Braga, D.; Mazzeo, P. P.; Ventura, B. *Dalton Trans.* **2012**, *41*, 531−539. (e) Roppolo, I.; Celasco, E.; Fargues, A.; Garcia, A.; Revaux, A.; Dantelle, G.; Maroun, F.; Gacoin, T.; Boilot, J. P.; Sangermano, M.; Perruchas, S. *J. Mater. Chem.* **2011**, *21*, 19106−19113. (f) Perruchas, S.; Desboeufs, N.; Maron, S.; Le Goff, X. F.; Fargues, A.; Garcia, A.; Gacoin, T.; Boilot, J. P. *Inorg. Chem.* **2012**, *51*, 794−798.

(12) (a) Chaux, F.; Frynas, S.; Laureano, H.; Salomon, C.; Morata, G.; Auclair, M.-L.; Stephan, M.; Merdès, R.; Richard, P.; Ondel, M.-J.; Henry, J. C.; Bayardon, J.; Darcel, C.; Jugé, S. *C. R. Chim.* **2010**, *13*, 1213−1226. (b) Kaloun, E. B.; Merdés, R.; Genêt, J. P.; Uziel, J.; Jugé, S. *J. Organomet. Chem.* **1997**, *529*, 455−463.

(13) Demas, J. N.; Crosby, G. A. *J. Phys. Chem.* **1971**, *75* (8), 991−1024.

(14) Otwinowski, Z.; Minor, W. Processing of X-ray Diffraction Data Collected in Oscillation Mode. *Methods in Enzymology*; Carter, C. W., Jr., Sweet, R. M., , Eds.; Academic Press: New York, **1997**; Vol. *276*, Macromolecular Crystallography, Part A, 307−326.

(15) Altomare, A.; Cascarano, G.; Giacovazzo, C.; Guagliardi, A. *J. Appl. Crystallogr.* **1993**, *26* (3), 343−350.
(16) (a) Sheldrick, G. *Acta Crystallogr., Sect. A* **2008**, *64* (1), 112−122. (b) Sheldrick, G. M. *SHELX-97*; Göttingen University: Göttingen, Germany, 1997.
(17) (a) Flack, H. *Acta Crystallogr., Sect. A* **1983**, *39* (6), 876−881. (b) Flack, H. D. *Helv. Chim. Acta* **2003**, *86* (4), 905−921. (c) Flack, H. D.; Bernardinelli, G. *J. Appl. Crystallogr.* **2000**, *33* (4), 1143−1148.
(18) Putnam, C. D.; Hammel, M.; Hura, G. L.; Tainer, J. A. *Q. Rev. Biophys.* **2007**, *40*, 191−285.
(19) Farrugia, L. *J. Appl. Crystallogr.* **1997**, *30* (5 Part 1), 565.
(20) Medina, I.; Mague, J. T.; Fink, M. J. *Acta Crystallogr., Sect. E* **2005**, *61*, m1550−m1552.
(21) Herberhold, M.; Akkus, N.; Milius, W. *Z. Anorg. Allg. Chem.* **2003**, *629*, 2458−2464.
(22) Arkhireeva, T. M.; Bulychev, B. M.; Sizov, A. I.; Sokolova, T. A.; Belsky, V. K.; Soloveichik, G. L. *Inorg. Chim. Acta* **1990**, *169*, 109−118.
(23) Churchill, M. R.; Rotella, F. J. *Inorg. Chem.* **1977**, *16*, 3267−3273.
(24) Kitagawa, H.; Ozawa, Y.; Toriumi, K. *Chem. Commun.* **2010**, *46*, 6302−6304.
(25) Lobana, T. S.; Kumar, R.; Sharma, R.; Nishioka, T.; Castineiras, A. *J. Coord. Chem.* **2005**, *58*, 849−855.
(26) Stepnicka, P.; Gyepes, R.; Podlaha, J. *Collect. Czech. Chem. Commun.* **1998**, *63*, 64−74.
(27) Tard, C.; Perruchas, S.; Maron, S.; Le Goff, X. F.; Guillen, F.; Garcia, A.; Vigneron, J.; Etcheberry, A.; Gacoin, T.; Boilot, J.-P. *Chem. Mater.* **2008**, *20*, 7010−7016.
(28) Kyle, K. R.; Ryu, C. K.; Dibenedetto, J. A.; Ford, P. C. *J. Am. Chem. Soc.* **1991**, *113*, 2954−2965.
(29) Harvey, P. D.; Knorr, M. *Macromol. Rapid Commun.* **2010**, *31*, 808−826.
(30) Vitale, M.; Ryu, C. K.; Palke, W. E.; Ford, P. C. *Inorg. Chem.* **1994**, *33*, 561−566.
(31) De Angelis, F.; Fantacci, S.; Sgamellotti, A.; Cariati, E.; Ugo, R.; Ford, P. C. *Inorg. Chem.* **2006**, *45*, 10576−10584.
(32) (a) Knorr, M.; Guyon, F.; Khatyr, A.; Strohmann, C.; Allain, M.; Aly, S. M.; Lapprand, A.; Fortin, D.; Harvey, P. D. *Inorg. Chem.* **2012**, *51*, 9917−9934. (b) Knorr, M.; Guyon, F.; Kubicki, M. M.; Rousselin, Y.; Aly, S. M.; Fortin, D.; Harvey, P. D. *New J. Chem.* **2011**, *35*, 1184−1188. (c) Knorr, M.; Guyon, F.; Aly, S. M.; Lapprand, A.; Khatyr, A.; Fortin, D.; Harvey, P. D. *J. Inorg. Organomet. Polym.* **2010**, *20*, 534−543. (d) Knorr, M.; Guyon, F.; Khatyr, A.; Strohmann, C.; Kubicki, M. M.; Rousselin, Y.; Aly, S. M.; Fortin, D.; Harvey, P. D. *Inorg. Chem.* **2010**, *49*, 5834−5844. (e) Guyon, F.; Khatyr, A.; Knorr, M.; Strohmann, C.; Aly, S. M.; Abd-El-Aziz, A. S.; Fortin, D.; Harvey, P. D. *Dalton* **2009**, 948−955.
(33) Johnson, G. E. *J. Phys. Chem.* **1974**, *78*, 1512−1521.